JOURNAL OF MATERIALS SCIENCE 25 (1990) 4301–4308

Characterization of fracture toughness of high strength low alloy steel weldments using stretch zone width measurements

M. R. BAYOUMI*
Mechanical Engineering Department, Faculty of Engineering, Assiut University, Assiut, Egypt

Most of the industrial applications involving use of high-strength low-alloy steels require good weldability. Thus it is important to characterize the properties of the welded steels, especially the heat affected zone. Attempts have been made to characterize the fracture toughness of the HAZ by the use of the J-integral and the crack opening displacement. In the present study, the effect of addition of titanium, vanadium and niobium, as well as combinations of these, on the fracture toughness of the heat affected zone of welded steel plates is examined. Six compositions were used in this study. Three-point bending specimens as well as tensile specimens were prepared. The fracture surfaces were examined in a scanning electron microscope to determine the fracture mode as well as the extent of the stretch zone as the crack blunts. Calculation of the fracture toughness parameter, J_{Ic}, is carried out through a quantitative stereofractographic analysis of the stretch zone at the crack tip. The results show that there is a marked increase in J_{Ic} due to the addition of the various alloying elements. Generally, the addition of niobium and titanium alone produce the highest J_{Ic} due to the extent of grain refinement that these elements produce.

1. Introduction

The major motivation for developments in high-strength low-alloy (HSLA) steels has been provided by the need for high strength, improved toughness ductility and formability as well as increased weldability. In order to meet these contradictory requirements, the carbon contents of the steels have been progressively lowered. The desired strength is largely produced by the additions of microalloying elements, such as aluminium, vanadium, niobium and titanium in combination with various forms of thermomechanical processing [1]. From the view point of fracture prevention of welded structures, it is significant and relevant to estimate accurately the fracture toughness of welded joints. Because in the weld bond region, mechanical properties and microstructures are inhomogeneous, it is important to determine if the fracture toughness parameter, for example K_{Ic}, J_{Ic} or critical crack opening displacement (COD), which are applicable to homogeneous materials, can be applied to estimate the fracture toughness of the weld bond region. Many parameters, for example the degree of inhomogeneity, crack location (heat affected zone, weld metal, base metal or a combination of these) specimen size, etc., may influence the fracture toughness of welded joints [2–6]. Because of the specific requirement of good weldability associated with the high-strength low-alloy steels, the fracture toughness of the heat affected zone (HAZ) is of considerable importance in most of the applications. The fracture toughness of these steels has been mainly characterized using elastic–plastic criteria. Considerable effort has been undertaken in recent years for characterization, both from the macroscopic and microstructural aspects of the fracture toughness on metallic materials. In particular, research has recently concentrated on development of criteria for these materials which accurately describe their behaviour as a function of testing parameters. Of these criteria, the use of the J-integral, which is well-suited for describing elastic–plastic behaviour, has been predominant. The method of determining the J-resistance curves to determine the onset of stable crack propagation has been standardized using partial unloading and compliance measurement procedures [7]. Other investigators have determined J_{Ic} under quasi-static as well as dynamic loading conditions as

TABLE I Chemical composition of the steels (wt %)

Steel	C	Si	Mn	P	S	Al	Nb	V	Ti
1	0.12	0.21	1.27	0.01	0.01	0.02	–	–	–
2	0.13	0.15	1.15	0.01	0.01	0.04	–	0.09	–
3	0.12	0.21	1.12	0.01	0.01	0.02	–	–	0.08
4	0.11	0.21	1.3	0.01	0.01	0.05	–	0.07	0.07
5	0.01	0.24	1.17	0.01	0.01	0.04	0.04	0.04	0.05
6	0.12	0.14	1.15	0.01	0.01	0.02	0.1	–	–

NB: The nitrogen and oxygen content in all steel groups is less than 0.006% and 100 p.p.m., respectively.

Present address: Department of Production Engineering and Mechanical System Design, Faculty of Engineering, King Abdulaziz University, Jeddah P.O. Box 9027, Saudi Arabia.

0022–2461/90 $03.00 + .12

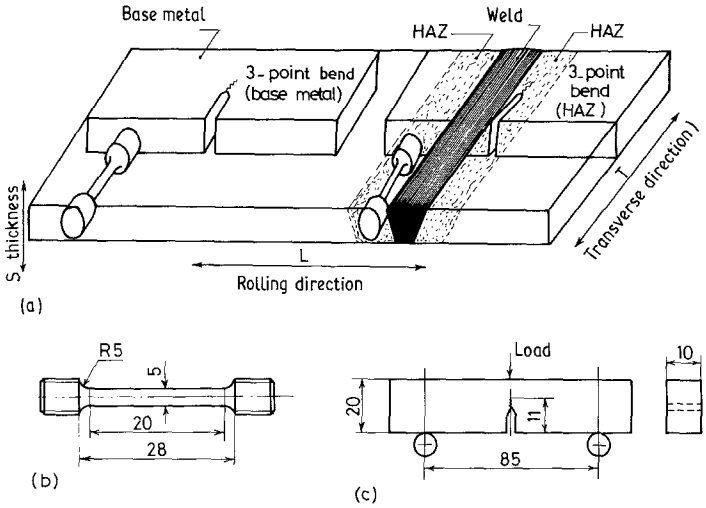

Figure 1 Location and dimensions of tensile and fracture specimens. (a) Location of different specimens, (b) tensile specimen dimensions, (c) three-point bending specimen dimensions.

a function of temperature in Charpy-size specimens for the purpose of developing an inexpensive and simple approach for measurement of J_{Ic} in engineering materials [8]. Because the stretch zone width is indicative of the extent of plastic blunting at the crack tip, it offers an alternative method of determining a fracture toughness parameter that might be associated with J_{Ic} [9–13].

In this investigation, fracture parameters of the base metal and HAZ of six HSLA steels containing various concentrations of titanium, vanadium and niobium were obtained. Because of their high ductility, the J-integral was used in order to account for their elastic–plastic behaviour. The toughness was determined using two different approaches, namely the J-resistance curve method, and mostly, from measurements of the stretch zone width on the same specimens after fracture, using scanning electron microscopy. The objective was to characterize the fracture toughness of the base metal and HAZ of the weldments with particular attention to the effects of microalloying additions. Also, the use of the stretch zone width as an alternative estimate of fracture toughness of the weldments was an important goal.

2. Experimental procedures

2.1. Material and welding procedures

The compositions of the six alloys used in this study are given in Table I. The compositions of the six metal groups are virtually the same except that groups 2 to 6 contain various amounts of vanadium, titanium and niobium microalloy additions either alone or in combinations with each other. Metal 1 contained no added vanadium, titanium or niobium and was used as a base metal reference. All the metal groups received the same hot-rolling treatment. Ingots of each 75 kg of each metal group were held at 1220° C for 2 h then reduced from 127 to 11.4 mm thickness by 15 successive straight hot-rolling phases. The final rolling pass was carried out at 800° C with the plates being air cooled to room temperature. The plates were then welded in a single pass using the submerged arc welding method. The chemical composition of the filler material (electrodes) as well as the welding condition used are shown in Table II. All the weldments were examined using an ultrasonic technique to determine the soundness of the weld.

2.2. Metallographic examination

The optical metallography performed on both etched and unetched samples from each weldment of the six metal groups, was used to identify the different weldment regions, as well as to categorize the material microstructure and to evaluate variations in the grain size and inclusion distribution.

2.3. Specimen preparation

Three types of specimen were prepared for evaluation in this study. Tensile and precracked three-point bending specimens were machined for tensile and fracture tests, while mounted fracture surface specimens were prepared for scanning electron microscopy. Tensile specimens from both the base metal and the HAZ from each of the metal groups were prepared.

TABLE II (a) Chemical composition (wt %) of the filler material (electrode) and (b) the welding conditions

(a)

Material	C	Mn	P	S	Si	Ni	Cr	No	V	Cu
Filler material (carbon steel)	0.07/0.15	0.85/1.25	0.03	0.035	0.15/0.35	–	–	–	–	0.3

(b)

Welding conditions			
Welding process	Submerged arc	Gap	2.4 mm
Current	525 A	Angle	60°
Voltage	28 V	Backing material	strip 12 6 mm thick
Welding seed	35 cm min^{-1}	Wire diameter	4 mm

These specimens were machined such that the gauge lengths were in the transverse direction with respect to the rolling direction as shown in Fig. 1a. These round tensile specimens were machined to dimensions and tolerances required by the ASTM standard E8-82 [14]. The dimensions are illustrated in Fig. 1b. Notched three-point bend specimens were prepared with the notch in both the base metal and the HAZ from each of the six metal groups. The position of the notch in the HAZ was determined using optical microscopy to ensure that for all the HAZ specimens, the crack will encounter the same microstructure as it propagates in the material. The three-point bend specimens were cut from the steel plates in the longitudinal transverse (L–T) orientation with respect to the rolling direction, as shown in Fig. 1a. The specimen dimensions were in accordance with the ASTM standard for J_{Ic} determination, ASTM E 813-81 [7]. These dimensions are illustrated in Fig. 1c. The specimens were fatigue precracked using a servo hydraulic testing machine according to ASTM E 813-81 procedure. The fatigue precracking, as well as the actual fracture tests, were carried out at room temperature. Finally, the fracture surfaces of the three-point bending specimens were cut with a high-speed abrasive cut-off saw, then these fracture surfaces were attached to aluminium holders to be examined using the scanning electron microscope.

2.4. Mechanical testing

The tensile tests were performed on a screw-type testing machine according to ASTM E8-82 specifications [14]. All the tensile testing was conducted at room temperature using a cross-head speed of 0.25 mm min^{-1}. The values of the ultimate strength, yield strength, fracture strain and the strain-hardening exponent were obtained for base metal and the HAZ of the six metal groups. The values of per cent elongation and reduction in area at fracture were obtained by measuring the gauge lengths and cross-sectional areas of the specimens before and after testing. Four specimens from both the base and HAZ from each metal group were tested. Adopting a single specimen technique to calculate the fracture toughness, J_{Ic}, the precracked three-point bend specimens were loaded at a quasi-static loading rate of 0.25 mm min^{-1} until noticeable stable crack growth occurred and maximum load has been reached on a load–stroke plot. The specimens were then broken in half and the fracture halves were observed by scanning electron microscopy. Three fracture specimens were tested for both the base and HAZ of each metal under consideration.

2.5. Stretch zone measurements

Because the stretch zone is the transition zone between the end of the fatigue pre-crack and stable crack growth, which is characterized by an extensive plastic deformation prior to crack initiation, this zone can be distinguished between the fatigue pre-crack region and the stable crack growth region on scanning electron micrographs of the fracture surface. Considering that deformation prior to crack initiation takes place along 45° slip lines, the critical stretch zone width $(SZW)_c$ can be measured by tilting a fractured specimen through 45° and examining it in the scanning electron microscope. This is schematically shown in Fig. 2.

Assuming a symmetrical blunt crack, an equation relating the stretch zone width $(SZW)_c$ to the COD has been derived [15]. If AB in Fig. 2 is the critical stretch zone width, it can be shown that the stretch zone width and the critical crack opening displacement, COD_c, are given by

$$(SZW)_c = \left[\frac{d}{\cos(\theta - \delta)}\right]\frac{1}{G} \quad (1)$$

and

$$(COD)_c = \left(\frac{2d}{\cos\delta + \sin\delta}\right)\frac{1}{G} \quad (2)$$

where d is the measured length of the stretch zone on the micrographs, δ is the incident angle of the beam (tilt-angle), $\theta = 45°$, and G is the magnification. Under plane-strain conditions, the critical value of the J-integral (J_{ISZ}) is related to $(COD)_c$ by [16]

$$J_{ISZ} = m\sigma_{flow}(COD)_c \quad (3)$$

where σ_{flow} is the flow stress (average of 0.2% yield stress and ultimate tensile stress) and m is a constraint factor due to plane strain loading which depends on material and testing variables [9, 12, 17] and is usually taken approximately equal to 2. Substituting Equation 2 into Equation 3 with $m = 2$, Equation 3 becomes

$$J_{ISZ} = \left(\frac{4\sigma_{flow}\, d}{\cos\delta + \sin\delta}\right)\frac{1}{G} \quad (4)$$

Halves of broken three-point bend specimens from both the base and the HAZ of each metal used in the J-resistance curve determinations were examined by scanning electron microscopy (Jeol JSM-840) using mostly a tilt angle $\delta = 30°$ and a magnification, G of about 100 to 250. The length of the stretch zone, d, was measured in at least ten locations in the plane strain region of the fracture surface and the results

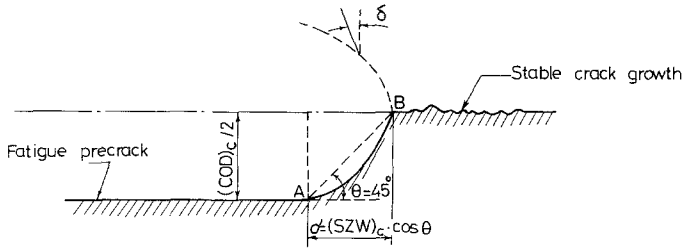

Figure 2 Illustration of the stretch zone on a precracked fracture surface [15].

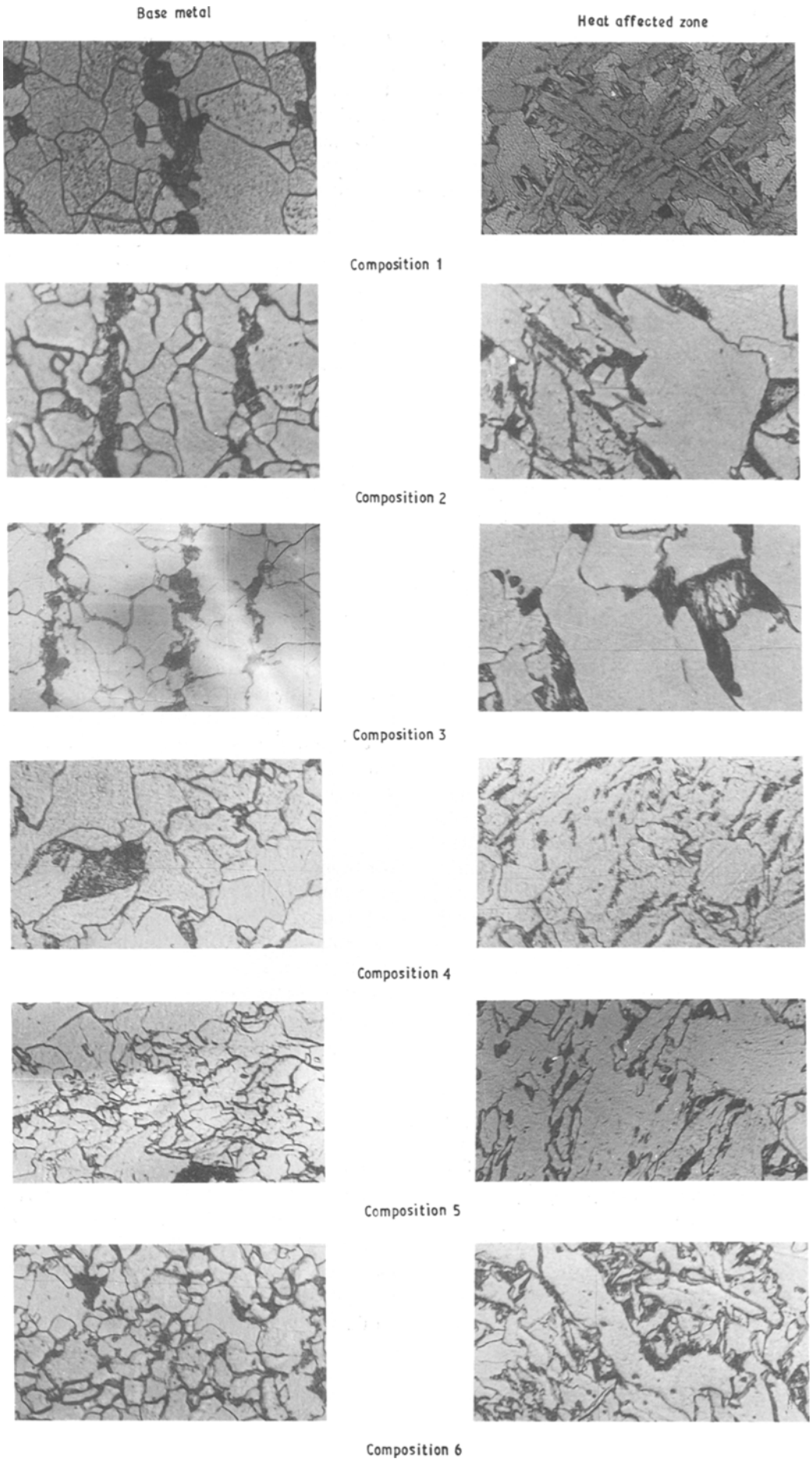

Figure 3 Microstructure of base metal at HAZ for the metal groups, × 800.

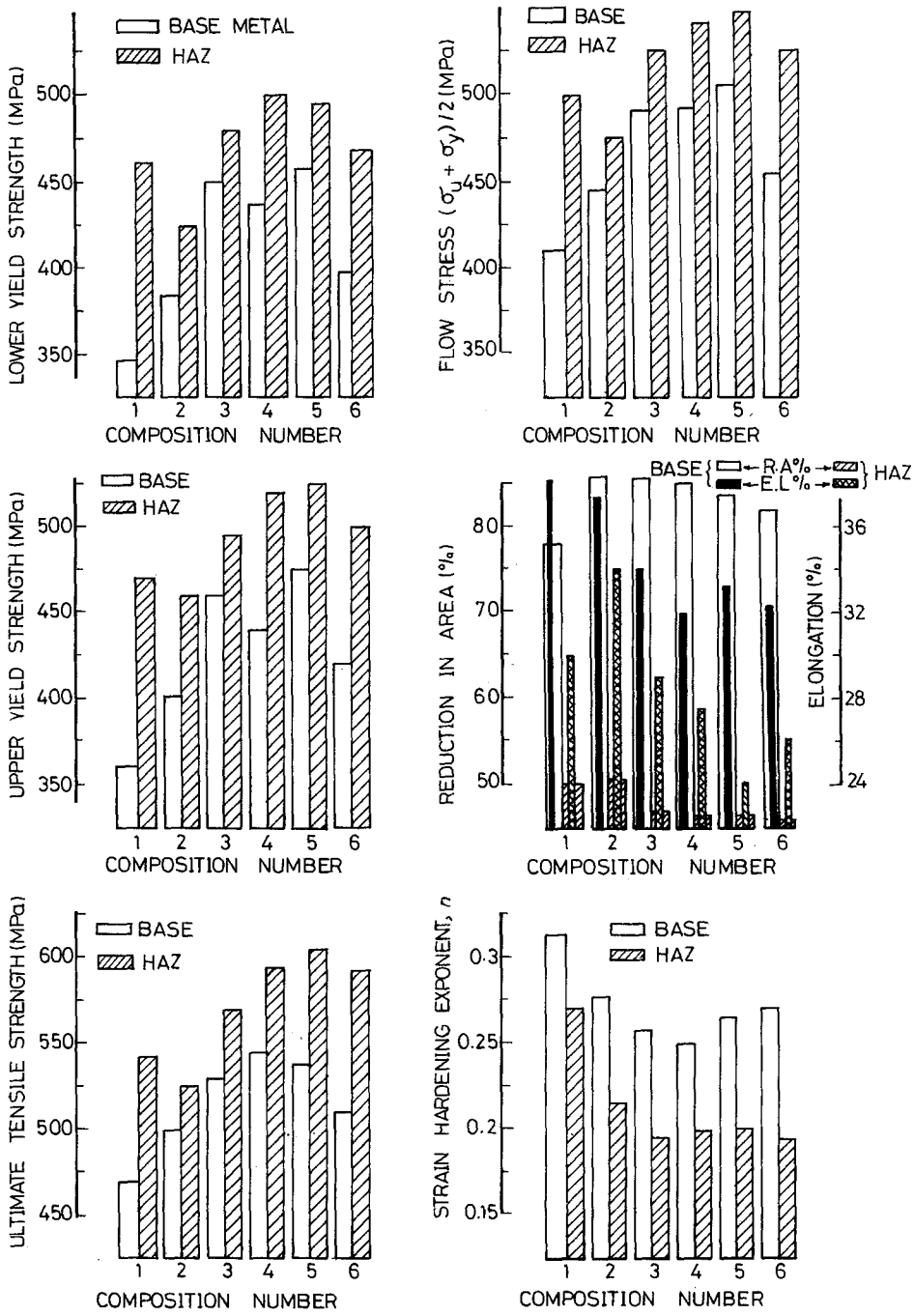

Figure 4 Variation of the mechanical properties in base metal and HAZ between the metal groups.

Composition no.	Alloying element		
	Nb	V	Ti
1	0.0	0.0	0.0
2	0.0	0.085	0.0
3	0.0	0.0	0.080
4	0.0	0.065	0.070
5	0.040	0.038	0.050
6	0.100	0.0	0.0

were averaged. The value of the fracture toughness J_{ISZ} was calculated using Equation 4.

3. Results and discussion

Fig. 3 shows the etched microstructure for the base metal and HAZ of the six metal groups. As indicated by this series of micrographs, a similar ferrite–pearlite microstructure exists for the base metal of all the metal groups. Also it is worth noting, concerning the microstructure, that the pearlite is directionally elongated, reflecting the influence of the controlled rolling, whereas the ferrite grains are virtually equiaxed. This figure also indicates that metal groups 3 and 6 have a significant improvement in grain refinement compared with the rest of the metal groups. The results obtained from the tensile testing for the base metal and the HAZ of the six metal groups are presented in Fig. 4, which shows the variations of the lower yield strength, the upper yield strength, the ultimate tensile strength, flow stress which is defined

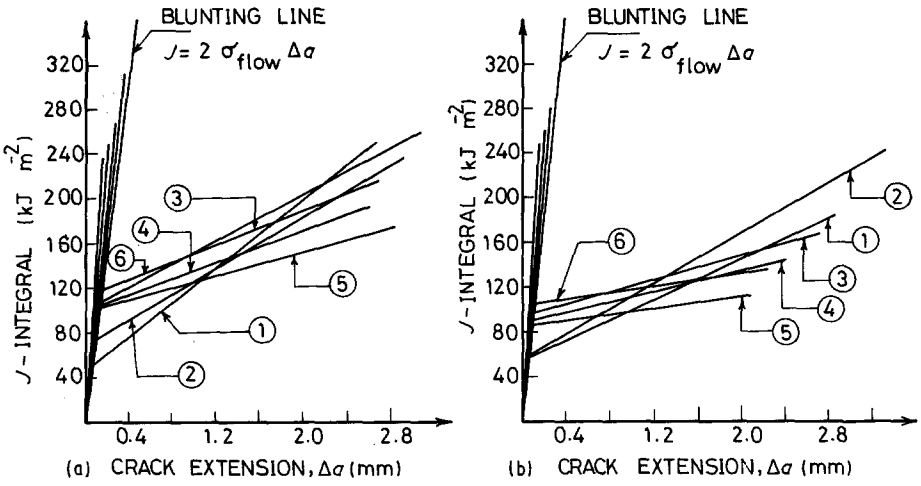

Figure 5 Resistance curves for the six metal groups. (a) Base metal, (b) HAZ.

as the average of the ultimate strength and the lower yield strength, the tensile ductility expressed as the per cent elongation and the per cent reduction in area as well as the strain hardening exponent. The J-resistance curves for both the base metal and the HAZ of the metal groups are shown in Figs 5a and b. Briefly, the J-integral is determined by the single specimen unloading compliance method, where a series of 10% unloading is performed to infer the crack extension, Δa, during the fracture test. The J-integral at each unloading was measured and a plot of the J-integral against Δa gives the J-resistance curve, and the intersection of the two lines of the J-resistance curve (the blunting line and the crack advance line) yields the value of J_{Ic}. The values of J_{Ic} for the base metal and the HAZ as determined from the J-resistance curves are shown in Fig. 6. It is noted that metals 3 and 6 possess the highest values of the fracture toughness, J_{Ic}. The variations of the stretch zone width $(SZW)_c$ and the critical value of the J-integral (J_{Ic}) among the base metal and the HAZ of the weldments of the metal groups are shown in Figs 7 and 8, respectively, while a typical scanning electron micrograph for the SZW region is shown in Fig. 9. These figures show that the maximum values of J_{Ic} are found in the base metal and HAZ of metals 3 and 6.

In the fracture characterization of the weldments, there seems to be a general agreement between the results obtained by the J-resistance curve method and those obtained from measurements of the stretch zone width. However, the values of J_{Ic} deduced from the stretch zone measurements are, in general, 15% to 30% higher than those obtained by the J-resistance curve method. These findings are similar to those reported previously [9, 15, 17] for both AISI 1045 steel and AISI 4340 steel. This may be due to the use of a constant value for the constraint m, namely $m = 2$ in Equation 3 for all the metal groups for both the base metal and HAZ. This assumption $(m = 2)$ was previously justified by finite element calculations [16]. Values of m in the present experiments for both the base metal and the HAZ of the six metal groups are presented in Fig. 10.

Small alloy additions of niobium, vanadium and titanium have been used in HSLA steels to improve tensile properties by precipitation strengthening [18].

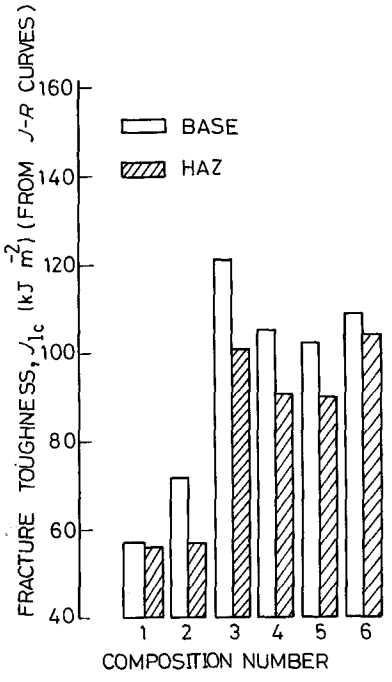

Figure 6 Variations of J_{Ic} in metal groups as determined from J-resistance curves.

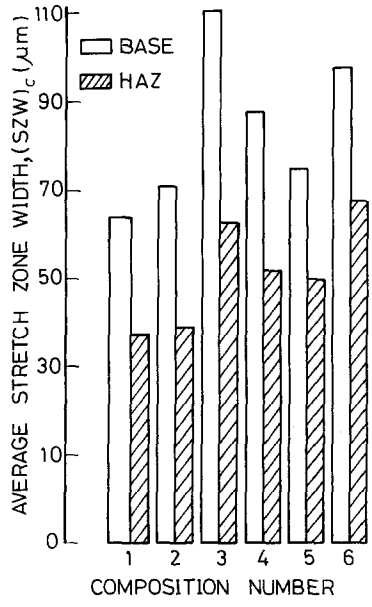

Figure 7 Variations of stretch width zone in the metal groups.

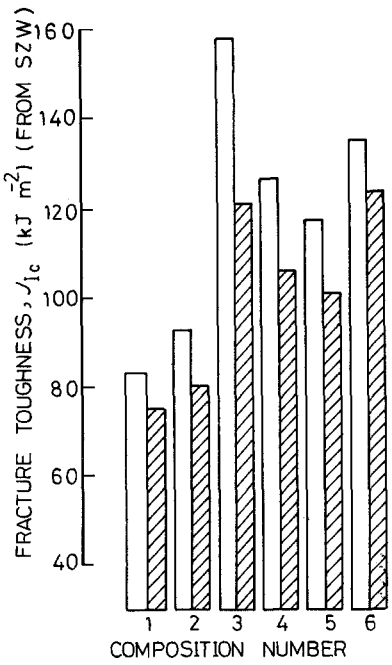

Figure 8 Variations of J_{Ic} in metal groups as determined from stretch zone width.

The excellent fracture toughness properties of pre-cracked bend specimens in both the base metal and the HAZ of weldments was shown to be dependent upon the alloy content. The reason attributed to the improved fracture toughness and grain refinement properties of niobium and titanium (metals 3 and 6) compared to vanadium (metals 4 and 5) is that niobium and titanium are less soluble in solid solution at high temperatures than is vanadium [19–21]. The result is that with heating and controlled rolling, niobium and titanium will precipitate in the form of Nb (C, N) and Ti (C, N) precipitates and pin the grain substructure to slow recrystallization and growth of austenite grains. Upon cooling, this structure results in smaller grain sizes. Vanadium is more soluble at high temperature and therefore does not precipitate during austenite recrystallization in these steel compositions [22]. The result is that recrystallization and grain growth occurs to greater extent and larger ferrite grains are thus produced upon cooling, leading to lower tensile and fracture toughness values.

4. Conclusions

The effect of alloying elements on the fracture toughness of HSLA weldment was studied. The fracture toughness parameter, J_{Ic}, was determined from J–resistance curves and from the measurements of the stretch zone width. Both techniques agree in showing the effect of alloying elements on the fracture toughness of weldments. Thus the stretch zone width is shown to be an effective back-up technique for charac-

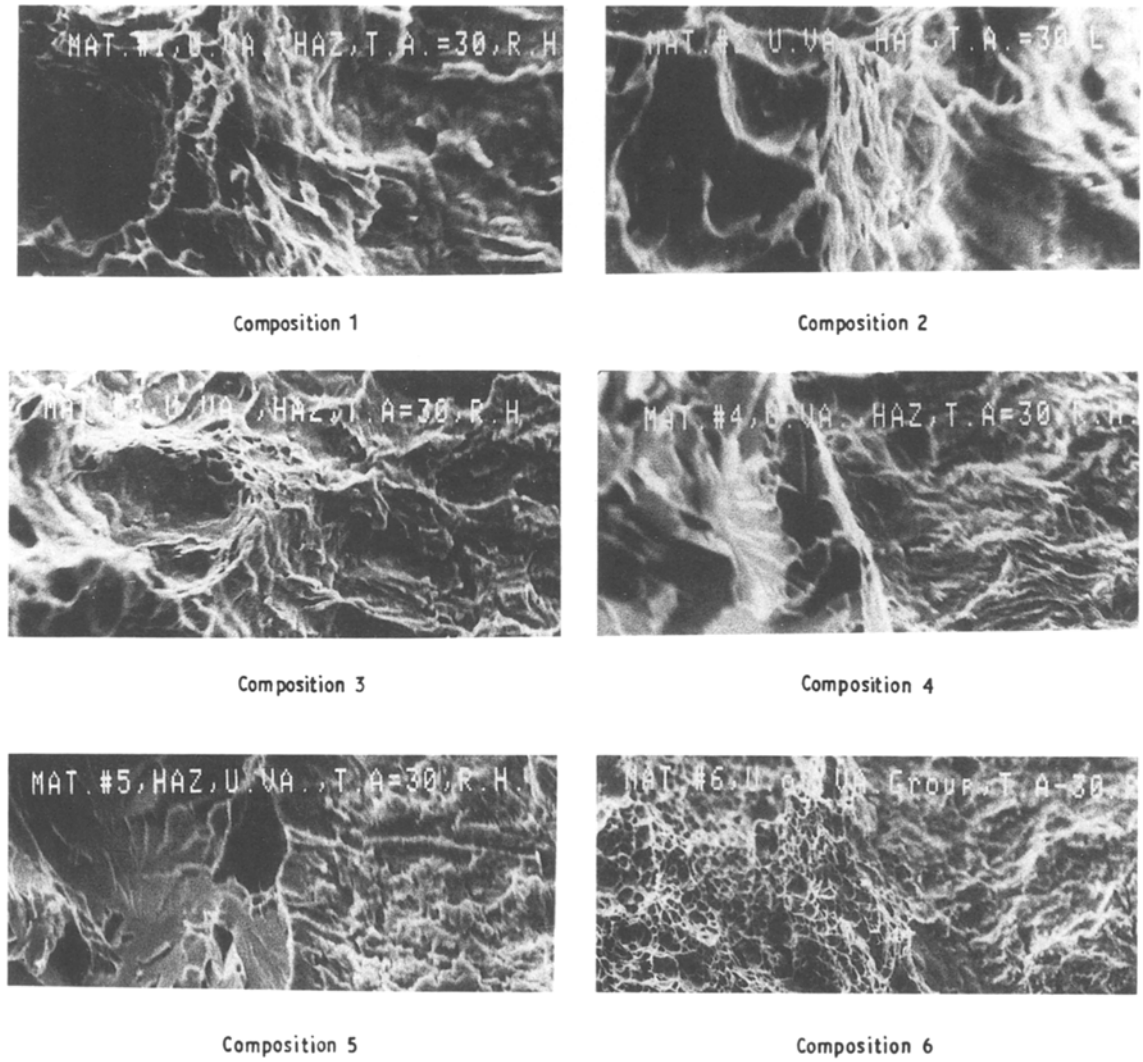

Figure 9 Scanning electron micrographs of fracture surfaces showing the stretch zone region in the HAZ, × 158.

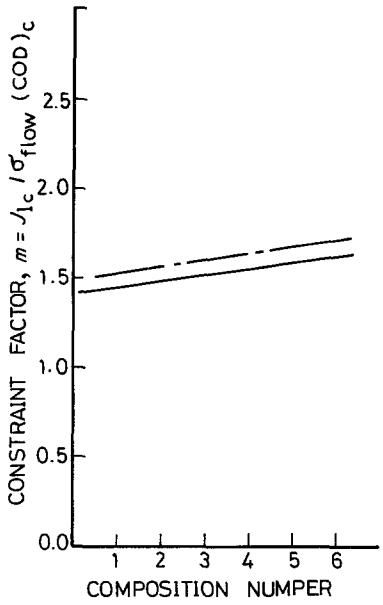

Figure 10 Variation of the constraint factor (in plane strain loading) with composition number. (——) Base metal, (- - -) HAZ.

terization of the fracture of weldments. Weldments with alloying elements of titanium and niobium possess the highest fracture toughness values.

References

1. F. B. PICKERING, "Physical Metallurgy and the desigr of Steels" (Applied Science, London, 1978).
2. F. M. BURDEKIN, M. G. DAWES, G. L. ARCHER, F. BONOMO and G. R. EGAN, *Brit. Weld. J.* **15** (1968) 590.
3. M. G. DAWS, *ibid.* **17** (1970) 533.
4. H. I. McHENRY and R. P. REED, *Weld. J.* **56** (1977) 1045.
5. K. IKEDA, M. AOKI, A. KIUCHI, N. OKUDA and N. TAKEUCHI, *J. Jpn Weld. Soc.* **46** (1977) 825.
6. H. TERADA and T. NAKAJIMA, *Int. J. Fract.* **27** (1985) 83.
7. "Standard Test for J_{Ic}, A Measure of Fracture Toughness", E 813-81 ASTM Annual Book of Standard, Part 10 (American Society for Testing and Materials, Philadelphia, Pennsylvania, 1981) pp. 810–16.
8. Committee on Rapid Inexpensive Tests for Determining Fracture Toughness, *Int. J. Fract.* **13** (1977) 227.
9. M. R. BAYOUMI and M. N. BASSIM, "Stretch Zone, Ductility and Toughness Studies in the Transition Region of 1045 Sted", in Proceedings of the International Conference of Materials ICM4, Stockholm, Sweden, Vol. 2 (1983) pp. 803–11.
10. A. J. KRASOWSKY and V. A. VAINSHTOK, *Int. J. Fract.* **17** (1981) 579.
11. P. DOIG, R. F. SMITH and P. E. J. FLEWITT, *J. Engng Fract. Mech.* **19** (1984) 653.
12. M. R. BAYOUMI, J. KLEPACZKO and M. N. BASSIM, *J. Test. Eval.* **12** (1983) 316.
13. Standard Method of Test for Elastic-Plastic Fracture Toughness J_{Ic} Recommended in Japan, JSME Standard, S 001-1981 (1981).
14. "Standard Methods of Tension Testing of Metallic Materials", E8-82, ASTM Annual Book of Standards (American Society for Testing and Materials, Philadelphia, Pennsylvania, 1983).
15. P. NGUYEN-DUY and S. BAYARD, *J. Engng Mater. Technol.* **103** (1981) 55.
16. M. G. DAWES, "Elastic-Plastic Fracture Toughness Based on the COD and J-Contour Integral Concepts", in "Elastic-Plastic Fracture", ASTM STP 668 (American Society for Testing and Materials, Philadelphia, Pennsylvania, 1979) pp. 307–17.
17. K. F. AMOUZOUVI and M. N. BASSIM, *J. Mater. Sci. Engng* **55** (1982) 257.
18. J. R. GUIMANAES, K. K. CHAWLA, P. R. ROIS and J. M. RIGSBEE, *Metals Technol.* **11** (1984) 1.
19. J. N. GOREDA and R. E. HOOK, *Metall. Trans. A* **1** (1970) 111.
20. L. J. CUDDY, *ibid.* **152** (1984) 87.
21. R. J. KLASSEN, M. N. BASSIM, M. R. BAYOUMI and H. G. F. WILSDORF, *Mater. Sci. Engng.* **80** (1986) 25.
22. M. G. AKBEN, I. WEISS and JONAS, *Acta Metall.* **29** (1981) 11.

Received 20 July 1988
and accepted 24 July 1989